SAND2019-5837C

Sandia BUCCX Titanium and Aluminum Sleeve Experiments

David E. Ames, Gary A. Harms, John T. Ford, Rafe D. Campbell

Sandia National Laboratories, P.O. Box 5800, Albuquerque, NM 87185
deames@sandia.gov, gaharms@sanida.gov, jtford@sandia.gov, rcampbe@sadia.gov

INTRODUCTION

The Sandia Critical Experiments Program provides a specialized facility for performing water-moderated critical experiments for pin-fueled cores. A history of safe reactor operations and flexibility in fuel types and reactor core configurations has resulted in the completion of multiple sets of benchmark experiments that have been published in the International Criticality Safety Benchmark Evaluation Project (ICSBEP) Handbook [1]. The program includes two different fuel options: the Seven Percent Critical Experiment (7uPCX) and the Burnup Credit Critical Experiment (BUCCX). The 7uPCX was designed for validating reactor physics methods and models for fuel enrichments greater than 5% ^{235}U [2]. The BUCCX was designed for inserting fission product materials to measure reactivity effects. Both are uranium oxide fueled but differ in enrichment, material properties, geometry, and array configuration. The set of experiments described here were performed using the BUCCX to determine the reactivity effects associated with introducing titanium and aluminum sleeves. A previous set of experiments measuring reactivity effects of titanium and aluminum rods was performed using the 7uPCX and is documented as LEU-COMP-THERM-097 [1].

A set of benchmark experiments with Rhodium foils has been completed using the BUCCX and documented as LEU-COMP-079 [1]. The experiments described here are similar, but without Rhodium present and with titanium or aluminum sleeves centered around selected fuel rods in the core. The experiments are designed to provide criticality safety benchmarks with significant reactivity from titanium and equivalent configurations with aluminum sleeves.

DESIGN OF THE CRITICAL ASSEMBLY

The assembly core resides in an elevated assembly tank that is connected to a moderator dump tank located at a lower elevation. The moderator resides in the dump tank when not in operation. To begin operations the moderator is pumped from the dump tank into the assembly tank. The moderator can be released by gravity to the dump tank through two large-diameter pneumatically operated dump values. The moderator is maintained at a constant temperature by a heater in the dump tank. During operation, the moderator is continually circulated between the dump tank and the assembly tank. The moderator level is maintained by overflow into a standpipe. Figure 1 provides an overall schematic of the critical assembly.

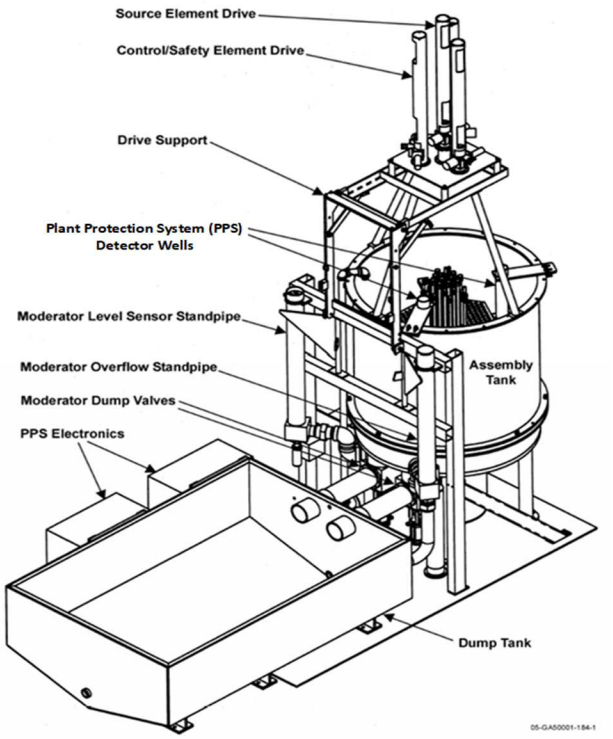

Fig. 1. Schematic of the critical assembly.

The fuel rods are supported by two 2.54 cm thick aluminum grid plates. The grid plates are located in the assembly tank to provide a 16.51 cm thick water reflector below the lower grid plate. The diameter of the tank provides a radial water reflector around the assembly that is at least 15.24 cm thick. The assembly tank standpipe is set to provide a 15.24 cm thick upper reflector when the assembly tank is full. The grid plates were fabricated with the holes on a 2.79908 cm triangular pitch and has 271 available fuel element positions.

The fuel rods are clad in Zircoloy-4 tubes with upper and lower end caps welded into place. UO_2 fuel pellets enriched 4.306 percent with a diameter of 1.265 cm are stacked to a height of 49.213 cm within the cladding. A spring is present between the upper end cap and the fuel pellets to maintain vertical alignment.

The assembly has three identical fuel-followed control/safety elements, two operated as safety elements and one as a control element. During the experiments, all are held at their most reactive position with the absorber (B_4C) above the surface of the water, such that absorber does not affect the system. The fuel followers are designed to be nearly identical

to a fuel rod in the assembly. Polyethylene separates the absorber from the fuel followers. When fully raised the fuel followers are in the core, the polyethylene-filled sections are above the upper grid plate and the absorber sections are above the level of the moderator.

During approach-to-critical experiments, the assembly is driven by a small stainless-steel-clad ^{252}Cf source that is located outside the grid plates. The behavior of the neutron population in the assembly is monitored by several fission chambers located outside the fuel array either in dry wells or outside the assembly tank. Two of the detectors inside the tank are in dry wells surrounded by polyethylene and provide signals to the assembly plant protect system (PPS).

EXPERIMENT SLEEVES

The experiment sleeves were fabricated from either Grade 2 titanium [3] or 6061-T6 aluminum [4] with a nominal outside diameter of 2.54 cm, wall thickness of 0.0889 cm, and length of 49.784 cm. The sleeves are approximately the same length as the fueled section of the fuel rods and have an inner diameter that is 1.0693 cm larger than the fuel rods. This allows for each sleeve to be centered around a fuel rod between the grid plates within the array. Bottom and top centering pieces fabricated from polyethylene were used to ensure the sleeves were uniformly centered around the fuel rods. Standard O-rings were used to hold the centering pieces in place. The sleeves had two 0.508 cm diameter holes near the ends to ensure moderator filled and drained from the sleeves effectively. Figure 2 shows two sleeves, one with the polyethylene centering piece inserted.

The mass, outside diameter, length and drain hole diameter of each experiment sleeve were measured. Using these data and the density of the sleeve material the inner radius of each sleeve was calculated.

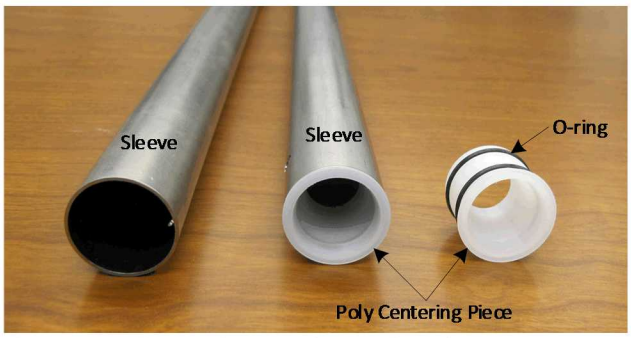

Fig. 2. Experiment sleeve and centering piece.

EXPERIMENT METHOD

The focus of these critical experiments was to measure the effects of titanium and aluminum sleeves in the fuel array on the critical array size. Every experiment with titanium sleeves has a corresponding experiment with aluminum sleeves in the same configuration though the numbers of fuel rods in the array differ because of the differing effects of titanium and aluminum.

The critical array size for each configuration was determined in an approach-to-critical experiment with the number of fuel rods in the array as a free parameter. The inverse count rate at successive fuel configurations for two detectors as a function of number of fuel rods was extrapolated to zero to obtain an estimate of the critical array size. During all measurements the control and safety elements were in their fully withdrawn or most reactive positions. Because the assembly tank was full of moderator during the measurements, the fuel rod array was fully reflected.

The triangular-pitched arrays were loaded from the center toward the outside while maintaining a roughly cylindrical cross section of the array. The loading order was identical for each experiment. Each fuel rod was in the same array location in every configuration that included that fuel rod.

For all configurations, a final approach-to-critical experiment was performed in which count rate measurements were taken for specific fuel arrays. At near delayed critical conditions, the fuel rods were added one at a time on the periphery of the array in a pattern that maintained symmetry as best as possible. A linear fit to the inverse count rate as a function of number of fuel rods in the array was extrapolated to zero inverse count rate to estimate the critical configuration of the experiment. The extrapolated critical array sizes were developed from inverse count rate data measured during these final experiments.

EXPERIMENTAL CONFIGURATIONS

Seventeen critical experiments were performed. Case 1 contained no experiment sleeves. Cases 2 through 9 included various numbers and arrangements of titanium sleeves. Case 2 had the most titanium present with 60 sleeves. Figure 3 is a photograph of the critical configuration for Case 2 with the red dots showing the 60 locations of the titanium sleeves. Case 9 had the least titanium with six sleeves. Cases 5 and 6 both had 36 sleeves but differed by the locations each occupied in the array. Cases 10 through 17 were identical to Cases 2 through 9 respectively except that the titanium sleeves were replaced with aluminum sleeves. Details of the sleeve configurations in each case are available in LEU-COMP-THERM-099.

EXPERIMENTAL RESULTS

Seventeen fully-reflected configurations were addressed by the critical experiments described here. The fuel array in each configuration had a roughly circular cross section. Table I lists the seventeen cases with the number of titanium or aluminum sleeves and the reactivity worth introduced by the sleeves in each case. In the benchmark evaluation, some of the geometrical and material details of the experiments

were simplified to arrive at a benchmark configuration. The biases associated with the simplifications were added to the experimental k_{eff} for each configuration to arrive at the benchmark model k_{eff}. The benchmark model k_{eff} with its uncertainty for each configuration is also shown in Table I.

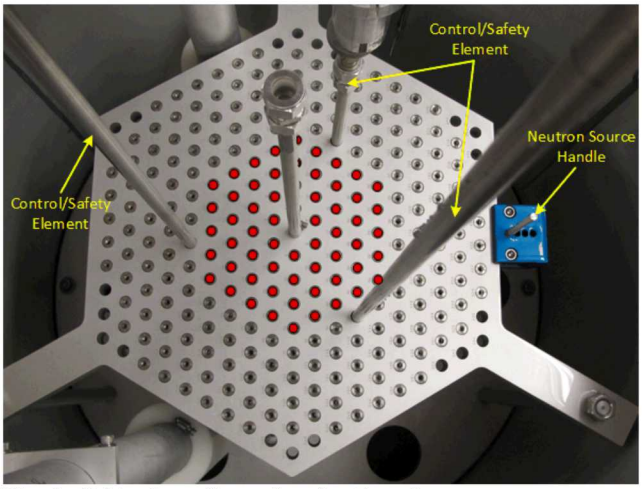

Fig. 3. Critical configuration for Case 2.

COMPARISON TO CALCULATION

Figure 4 shows the reactivity offset (ρ) of the MCNP6.2 [5] calculations using ENDF/B-VII.0 and ENDF/B-VII.1 cross sections. The error bars represent the stochastic uncertainties in the Monte Carlo calculations. The reactivity offset ρ is defined as

$$\rho = \frac{k_c - k_b}{k_c k_b} \quad (1)$$

where k_c is the calculated k_{eff} for the benchmark model of a given configuration and k_b is the evaluated benchmark model k_{eff} for the same configuration.

CONCLUSION

The BUCCX titanium and aluminum sleeve experiments reported here were designed to measure the effects of titanium on critical systems. The series of experiments provided criticality safety benchmarks with significant reactivity from titanium and equivalent configurations with aluminum sleeves. The experiments have been documented and approved for publication in the ICSBEP Handbook.

ACKNOWLEDGEMENTS

The critical experiments at Sandia are supported by the DOE Nuclear Criticality Safety Program. Sandia National Laboratories is a multimission laboratory managed and operated by National Technology & Engineering Solutions of Sandia, LLC, a wholly owned subsidiary of Honeywell International Inc., for the U.S. Department of Energy's National Nuclear Security Administration under contract DE-NA0003525.

Table I. Notable results for the critical experiments.

Case	Sleeves		Sleeve Reactivity Worth (%)	Fuel Rods	Benchmark Model k_{eff}
	Ti	Al			
1	0	0	0	132	1.00017 ± 0.00071
2	60	0	-9.57 ± 0.01	250	0.99965 ± 0.00083
3	54	0	-9.07 ± 0.01	240	0.99979 ± 0.00083
4	42	0	-7.67 ± 0.01	215	0.99964 ± 0.00083
5	36	0	-7.23 ± 0.01	209	1.00002 ± 0.00083
6	36	0	-6.23 ± 0.01	195	1.00054 ± 0.00083
7	24	0	-4.84 ± 0.01	177	0.99991 ± 0.00083
8	18	0	-4.67 ± 0.01	175	1.00055 ± 0.00083
9	6	0	-2.07 ± 0.01	148	0.99955 ± 0.00083
10	0	60	-0.31 ± 0.01	148	0.99909 ± 0.00071
11	0	54	-0.23 ± 0.01	147	1.00054 ± 0.00071
12	0	42	-0.13 ± 0.01	143	1.00051 ± 0.00071
13	0	36	-0.24 ± 0.01	143	1.00006 ± 0.00071
14	0	36	-0.02 ± 0.01	138	1.00000 ± 0.00071
15	0	24	-0.06 ± 0.01	137	0.99952 ± 0.00071
16	0	18	-0.15 ± 0.01	138	1.00037 ± 0.00071
17	0	6	-0.06 ± 0.01	134	1.00005 ± 0.00071

REFERENCES

1. "International Handbook of Evaluated Criticality Safety Benchmark Experiments." Paris: NEA 7360, OECD Nuclear Energy Agency, ISSN: 2618-0421, (2018).
2. "Reactor Physics and Criticality Benchmark Evaluations for Advanced Nuclear Fuel, Final Technical Report." TDR-30000849-000, Areva Federal Services, LLC (2008).
3. "Standard Specification for Seamless and Welded Titanium and Titanium Alloy Tubes for Condensers and Heat Exchangers," ASTM B338-10, ASTM International, West Conshohocken, PA (2010).
4. "Standard Specification for Aluminum and Aluminum-Drawn Seamless Tubes," ASTM B210-12, ASTM International, West Conshohocken, PA, (2012).
5. C.J. WERNER (editor), "MCNP Users Manual – Code Version 6.2", Los Alamos National Laboratory, report LA-UR-17-29981 (2017).

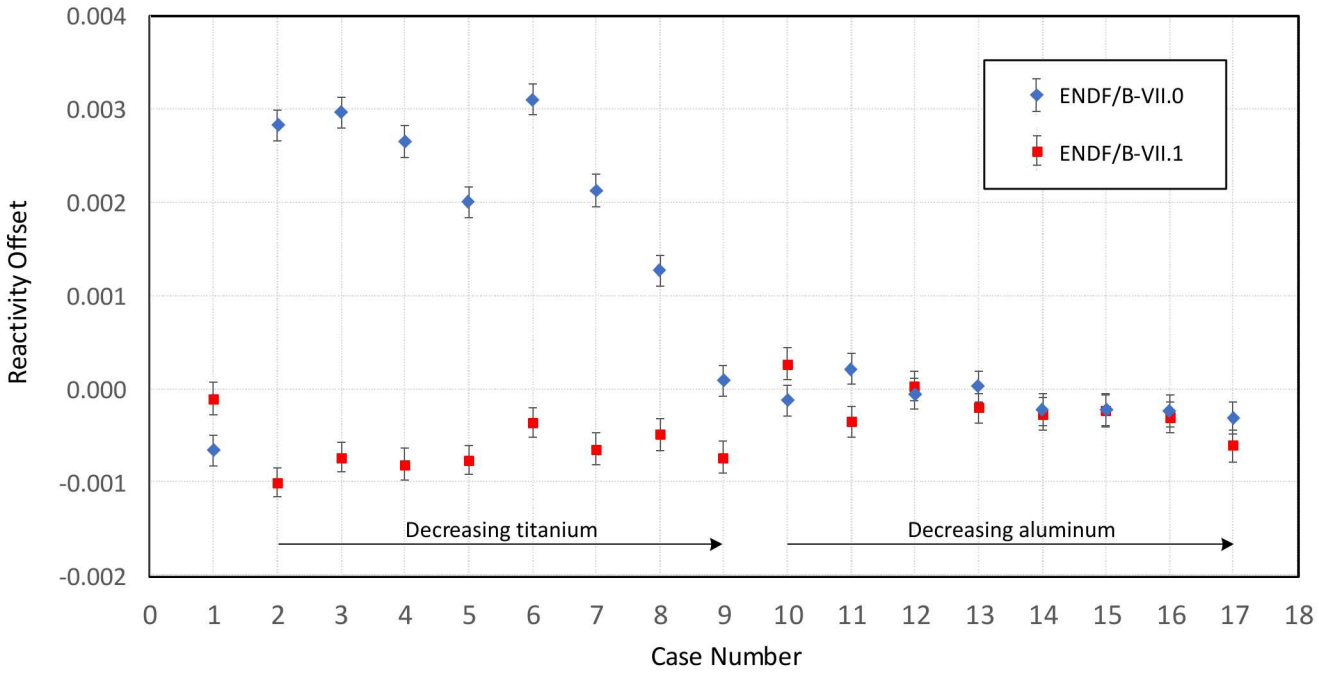

Fig. 4. Reactivity offset for the MCNP6.2 calculations using ENDF/B-VII.0 and ENDF/B-VII.1 cross sections.